Integrative Biology

Intratumoral Phenotypic Heterogeneity as an Encourager of Cancer Invasion

Journal:	*Integrative Biology*
Manuscript ID:	IB-ART-02-2014-000022.R1
Article Type:	Paper
Date Submitted by the Author:	24-Apr-2014
Complete List of Authors:	Shin, Yoojin; Korea University, Department of Mechanical Engineering Han, Sewoon; Korea University, Department of Mechanical Engineering Chung, Euiheon; Gwangju Institute of Science and Technology, Department of Mechatronics & Department of Medical System Engineering Chung, Seok; Korea University, Department of Mechanical Engineering

To study cancer heterogeneity, most research has focused on molecular and genetic associations. However, the lack of properly controlled in vitro cancer models has limited our understanding of the role of heterogeneous cancer cell subpopulations in tumor progression and invasion. In this study, we present a novel in vitro breast tumor model to mimic intratumor heterogeneity in a microfluidic system capable of providing physiologically relevant tumor microenvironment for cancer cells by incorporating ECM scaffolds. With this system, we suggest that interactions between subpopulations of cancer cells with distinct characteristics promote tumor progression and invasion. This intratumor heterogeneity model will allow new insights into phenotypic event of heterogeneous cancer cell subpopulations during invasion.

Intratumoral Phenotypic Heterogeneity as an Encourager of Cancer Invasion

Yoojin Shin[1], Sewoon Han[1], Euiheon Chung[2,3], and Seok Chung[1*]

Authors' Affiliations: [1]Department of Mechanical Engineering, Korea University, South Korea; [2]Department of Mechatronics, Gwangju Institute of Science and Technology, Gwangju, South Korea; [3]Department of Medical System Engineering, Gwangju Institute of Science and Technology, Gwangju, South Korea

Corresponding Author: Seok Chung, Department of Mechanical Engineering, Korea University, #512B, Innovation Hall, Anam, Seongbuk, Seoul, 136-713, South Korea, Phone:+82-2-3290-3352, Fax: +82-2-926-9290, E-mail: sidchung@korea.ac.kr

Keywords: intratumor heterogeneity, cancer invasion, extracellular matrix, microfluidic system, 3D co-culture

Abstract

We present a novel *in vitro* breast tumor model to mimic intratumoral phenotypic heterogeneity based on a microfluidic sysftem incorporating ECM scaffolds capable of providing a physiologically relevant tumor microenvironment. To study the regulation of invasive potentials by intratumoral subpopulation conditions, we developed heterogeneous cancer cell subpopulations by co-culturing two breast cancer cell types with distinct phenotypes, specifically, highly invasive and epithelial-like cancer cells. Our results indicate that intratumoral phenotypic heterogeneity acts as an encourager of cancer cell invasion through a 3D matrix depending on the neighboring ECM, with highly invasive cancer cells acting as the 'leader' and epithelial-like cancer cells as the 'follower', therefore enhancing metastatic potential.

Introduction

Cancer heterogeneity, documented since the early days of cancer research(1), is an important aspect of tumor progression and a clinically significant factor(2). The tumor microenvironment consists of heterogeneous cell types, including not only cancer cells but also stromal cells, such as fibroblasts and vascular cells. The critical roles of stromal cells in tumor growth and invasion (prerequisite steps of metastasis) are recognized, both *in vitro* and *in vivo*(3, 4). Heterogeneous cancer cell subpopulations with dissimilar characteristics, designated "intratumor heterogeneity", co-exist, even within a single tumor(5).

Intratumor heterogeneity has been identified and actively investigated with technological advances in recent years, leading two emerging conceptual frameworks: clonal evolution and cancer stem cell hypothesis(1, 6). The majority of tumors display heterogeneous characteristics. For example, tumors consist of cells with characteristically different subtypes displaying distinct molecular and gene expression patterns(7). Phenotypic heterogeneity, including cellular morphology, drug resistance, and proliferative, invasive and metastatic potential(2, 8), leads to failure to predict the progression patterns of metastasis and consequently to select the most suitable treatment for patients(9, 10). During oncogenesis, intratumor heterogeneity is caused by both genetic and non-genetic factors, such as genetic mutations and abnormal microenvironment including activated stromal cells(11), hypoxia(12), and remodeled extracellular matrix (ECM)(13).

Clinical reports have revealed that intermixed cancer cell subpopulations with distinct genetic and phenotypic characteristics exist within a single tumor(14). There is evidence to suggest sub-specialization of cancer cells and their mutual support in tumor progression(7). To date, most research involving cancer heterogeneity has focused on molecular and genetic associations(15, 16). However, the role of heterogeneous cancer cell subpopulations in tumor progression and invasion has been overlooked due to the lack of properly controlled *in vitro* models. To clarify the mechanisms by which intratumor heterogeneity influences metastasis, and more specifically, how subpopulations of cancer cells within a tumor mutually interact during the invasion process, a well-controlled experimental system is required to precisely model complex cell-to-cell and cell-to-ECM interactions under well-defined heterogeneous cancer cell subpopulations. Here, we have presented a novel *in vitro* breast

tumor model to mimic intratumor heterogeneity by constructing a microfluidic system incorporating ECM scaffolds capable of providing a physiologically relevant tumor microenvironment. To investigate the influence of subpopulations of cancer cell on invasion, we composed the intratumor heterogeneity with cancer subpopulations that have the distinct degree of invasive potential: 1) highly invasive cancer cells (HIC), MDA-MB-231, with the high invasive potential and the capacity of proteolytic ECM remodeling, and 2) Epithelial-like cancer cells (ELC), MCF-7, which retain epithelial characteristics that presents a none-aggressive and low-invasive phenotype with strong cell-cell junction. These subpopulations of cells were co-cultured in a carefully controlled microfluidic environment in contact with various ECM scaffolds. Our results suggest that interactions between HICs and ELCs promote tumor invasion with HIC acting as the *leader* and ELC as the *follower*, and therefore influence metastatic potential.

Materials and Methods

Fabrication of the microfluidic system: A microfluidic device composed of PDMS (polydimethylsiloxane; Sylgard 184; Dow Corning, MI, USA) with four ECM scaffold regions and three main microchannels was fabricated with a SU-8 photoresist master (MicroChem, MA, USA) using a conventional soft lithography process. The PDMS-based microfluidic system was bonded onto a sterilized 24×24 cover glass using oxygen plasma (Femto Science, Korea) after autoclaving, and coated with poly-D-lysine hydrobromide (PDL, MW 30,000-70,000, Sigma-Aldrich, St Louis, MO). Collagen type I (rat tail; cat. no. 40236; BD Bioscience) or matrigel (growth factor reduced (GFR) Phenol Red-free; BD Bioscience) hydrogel was used as the ECM scaffold. Collagen solution was diluted to 2 mg/ml in 10X PBS and deionized water, and pH adjusted with 0.5 N NaOH to 11. ECM hydrogel was filled into and fixed in ECM scaffold regions with a micropipette, followed by incubation for 30 min at 37°C in a 5% CO_2 incubator for gelling. After gelation, all microchannels were filled with culture medium and incubated at 37°C in a 5% CO_2 incubator, prior to use.

Cell culture: MDA-MB-231 and MCF-7 breast adenocarcinoma cells were obtained from KCLB (Korea Cell Line Bank, Korea) and NCC (National Cancer Center, Korea), respectively. The two cell types were maintained in RPMI 1640 supplemented with 10% heat-inactivated fetal bovine serum (FBS, Gibco) and 1% penicillin/streptomycin (Gibco) at 37°C in 5% CO_2.

Heterogeneous cell culture in microfluidic system: Harvested cells were suspended in RPMI 1640 containing 1% FBS at the desired density (MCF-7:MDA-MB-231 = 2:1 or 10:1 of $2x10^6$ cells/ml total density), seeded into cell culture channels (center and right channels) of a microfluidic device and maintained in the tilted position at 37°C in a 5% CO_2 incubator for 2 h to allow cell attachment on the side of ECM (collagen or Matrigel) scaffold by gravity. For sequential heterogeneous cell culture, after the first seeded cells were perfectly attached on the ECM scaffold, second cells were seeded into cell culture channels and incubated in a similar manner. Following cell attachment, the condition channel was filled with RPMI 1640 containing 5% FBS supplement for generating the FBS gradient

within ECM scaffolds and two cell culture channels filled with the same medium containing 1% FBS supplement. The culture medium was refreshed daily.

Heterogeneous cell culture imaging: HICs (MDA-MB-231) were green fluorescence-labeled using the Vybrant® CFDA SE Cell Tracer Kit (Molecular Probes) to distinguish from MCF-7 before seeding into the microfluidic system. HICs (MDA-MB-231) were incubated with 10 μM CFDA SE in a 5% CO_2 incubator at 37°C for 15-20 min and washed twice with culture medium. After three days of cell culture, cancer cells invading collagen scaffolds in the microfluidic system were fixed with 4% (w/v) paraformaldehyde in PBS for 15 min and those invading matrigel scaffolds with 2% (w/v) paraformaldehyde in PBS for 20 min. Thereafter, both cell types were permeabilized with 0.1% Triton X-100 for 5 min at room temperature. Fixed and permeabilized cells were subjected to fluorescence staining with DAPI (blue, 40,6-diamidino-2-phenylindole; Sigma-Aldrich) for visualizing nuclei and rhodamine-phalloidin (red, Sigma-Aldrich) for actin filaments. Finally, HICs (MDA-MB-231) were stained green (CFDA) and red (rhodamine-phalloidin), and ELCs (MCF-7) stained red (rhodamine-phalloidin).

Functional blocking of E-cadherin with antibody: After seeding and allowing cell attachment to the ECM scaffolds, cells were cultured in RPMI 1640 containing 1% FBS in the presence of 5 μg/ml E-cadherin monoclonal antibody (SHE78-7, Novex®), and the medium containing 5 μg/ml SHE78-7 antibody changed daily for 3 days.

Immunocytochemistry: Cell fixation and permeabilization were carried out in a similar manner as described for heterogeneous cell culture imaging before blocking. Cells were blocked with Block ACE (DS Pharma Biomedical Co., Japan) for >1 h at room temperature and washed with PBS more than twice. Thereafter, 60 μl of 1:100 diluted primary antibody solution of anti-Claudin 5 (Abcam), anti-Claudin 1 (Abcam), anti-Occludin (Abcam), and E-cadherin (H-108) (Santa Cruz Biotechnology) in PBS was added to each microchannel and incubated at 4°C overnight. After washing with PBS, secondary Alexa Fluor® 488 Goat Anti-Rabbit IgG (H+L) (Molecular Probe) was added and

incubated at 4°C overnight. Thereafter, microchannels were washed with PBS on a shaker at 4°C overnight.

HICs extraction from ECM scaffolds: HICs invading ECM in the microfluidic system were extracted after culture for 3 days. HICs were removed from ECM by incubating with an extraction solution (0.5% Triton X-100, 20 mM NH_4OH in PBS) for 2 h, washed more than three times with culture medium, (17) and incubated at 37°C in a 5% CO_2 incubator overnight before use.

Laminin antibody staining for remodeled ECM: After HIC extraction, remodeled ECM were fixed with 2% (w/v) paraformaldehyde in PBS for 20 min. Following fixation, 60 μl of 1:100 diluted anti-Laminin antibody in PBS was added to each microchannel and incubated at 4°C overnight. Cells were washed with PBS and incubated with 1:100 diluted Alexa Fluor® 488 Goat Anti-Rabbit IgG (H+L) in PBS at 4°C overnight.

HIC-conditioned medium preparation: When HICs (MDA-MB-231) achieved 70~80% confluence in a 75cm^2 (T-75) flask, cells were incubated in serum-free RPMI 1640 for 48 h. Subsequently, HIC culture medium was harvested, centrifuged [at 1000rpm for 5 min], filtered with a 0.22 μm pore membrane, and mixed with fresh medium (HIC culture medium: fresh medium=1.5:1) and 5% FBS.

Quantification: Cells invading ECM were counted after nuclear staining with DAPI, and the number of cells on the side of the ECM scaffold determined by dividing the size of tumor mass by single cell size. The invading distance was quantified by measuring the distance of the furthest cell from the starting point. Moreover, the index of microtracks filled by cells was analyzed by dividing the total number of generated microtracks, paths in ECM scaffold through which HICs invaded, by the number of microtracks filled by cells.

Results and Discussion

HICs induce and lead 3D invasion of ELCs into Matrigel, but not type 1 collagen

We developed an *in vitro* microfluidic model of heterogeneous cancer cell subpopulation culture to mimic diverse intratumoral conditions and study the invasive potentials of various subpopulations. A specific microfluidic cell culture device incorporating the ECM scaffold was constructed to provide a physiologically relevant ECM microenvironment for cells. ELCs (MCF-7) were mono- or co-cultured with HICs (MDA-MB-231) labeled with green fluorescent dye on the side of the ECM scaffold under a fetal bovine serum (FBS) gradient **(Figure 1a)**. Both co-cultured ELCs/HICs and mono-cultured ELCs representing heterogeneous and homogeneous tumor populations, respectively, formed tumor masses on the side of the ECM scaffold. In the heterogeneous tumor mass, ELCs (MCF-7) and green fluorescent-labeled HICs (MDA-MB-231) were mixed and cultured on an ECM scaffold of collagen type 1 (COL) or Matrigel (MAT) at a seeding ratio of 2:1 (ELC:HIC) (total density of two million cells/ml) for three days in the presence or absence of a 5% FBS gradient.

The ability of HICs to promote ELC invasion in the heterogeneous tumor mass was strongly dependent on the ECM type. On COL, ELC invasion remained almost unchanged, both in the absence and presence of the FBS gradient, independent of co-culture with HICs **(Figure 1b)**. In contrast, on MAT, the number of ELCs invading the ECM was significantly increased upon co-culture with HICs (Co; co-culture in **Figure 1b**), compared to mono-culture (Mono; mono-culture in **Figure 1b),** both in the absence and presence of the FBS gradient. Heterogeneous tumor masses of ELC and HIC on MAT were generated using various seeding patterns (HICs introduced by [1] mixing directly with, [2] before, and [3] after MCF-7, and [4] MCF-7 only **(Figure 1a**)) at seeding ratios of 2:1 and 10:1 (ELC:HIC) in the absence or presence of FBS gradient. After three days, 3D invasion of ELCs into MAT from the heterogeneous tumor mass was increased, regardless of the relative position of HICs, whereas ELCs from the homogeneous tumor mass remained non-invasive **(Figure 1c)**. Quantification data (**Figure 1c and Supplementary Figure 1(a))** demonstrated that even a small proportion (10:1) of HICs effectively promoted ELC invasion.

A simple depiction of the 3D invasion of cancer cells into COL or MAT from hetero- or homogeneous tumor masses is presented in **Figure 2a**. To further investigate how HICs influence ELC invasion into ECM, ELCs and green fluorescence-labeled HICs were co-cultured on COL or MAT at a ratio of 2:1 (ELC:HIC). After three days of culture, F-actin of both cell types was stained with rhodamine phalloidin. Notably, ELCs in the homogeneous cancer mass remained non-invasive on the side of both COL and MAT scaffolds during the culture period (**Figure 2b**). When ELCs and HICs were co-cultured on COL, only HICs (green) invaded ECM while ELCs remained non-invasive (**Figure 2c, Supplementary Figure 1(b)**). However, upon co-culture on MAT, we observed increased total invasion of ELCs following HICs (**Figure 2d, Supplementary Figure 1(b)**). Interestingly, as shown in **Figure 2d**, HICs (green) were always at the front, while ELC displayed collective chain migration and invasion into MAT following HIC invasion (**Figure 2d**). F-actin (**Figure 2e, 2f**) and beta-1 integrin-stained cells (**Figure 2g**) in MAT clearly demonstrated that the leading HICs actively interact with ECM by forming filopodial and lamellipodial extensions (indicated with arrows in **Figure 2e**) and focal adhesions (indicated by beta-1 integrin (red) localization in cell-matrix adhesions in **Figure 2g**), whereas ELC followers passively invade ECM with no protrusions (**Figure 2f**) or focal adhesions (**Figure 2g**).

Microtracks generated by HICs in MAT promote ELC invasion

Matrix-dependent plasticity of cancer cells has been reported previously(18). We proposed that since COL had a fibrillar and porous structure, MDA-MB-231 cells individually invaded COL with focal adhesion-based extension of long lamellipodial and filopodial protrusions by squeezing through pores(18). On the other hand, since MAT had a denser structure, MDA-MB-231 cells invaded via proteolytic matrix degradation activity by generating microtracks within the matrix(18). The microtracks generated were examined by allowing HICs to migrate into the matrix for 3 days and extracting invaded cells. **Figure 3a** depicts COL and MAT after HIC extraction. Interestingly, microtracks were observed in MAT, but not COL. Microtracks in MAT were clearly visualized via antibody staining for laminin, a major component of Matrigel (**Figure 3b**). Green fluorescence is more

richly stained on the surfaces of microtracks (white arrows in **Figure 3b**) because the staining solution flowed through the microtracks and diffused into the remained region of matrigel scaffold. These findings indicate active ECM proteolysis by HICs and support their activity as a main 'leader' of ELC invasion. This role was confirmed by introducing ELCs on remodeled MAT (containing microtracks) and culturing under a 5% FBS gradient for three days. Some ELC cells migrated and proliferated along the microtracks, and extended their growth in the radial direction to the microtracks simultaneously, maintaining contact with the original tumor colony, as shown in **Figure 3c**. Few cells were detached from the tumor colony and migrated along the microtracks. Interestingly, other than the microtracks, ELCs never invaded MAT. The number of ELCs invading along the preformed microtracks was a quarter of those cultured with HICs (**Figure 3d**). The number of microtracks filled by ELCs was significantly lower upon mono-culture, compared to co-culture with HICs (**Figure 3e**). Our data suggest that the microtracks within MAT generated by HICs contribute to a proportion of ELC invasion, but are not sufficient to promote considerable ELC invasion.

The strong cell-cell adhesion required for epithelial maintenance in ELCs may prevent cellular invasion into microtracks. This hypothesis was examined by suppressing expression of E-cadherin, a calcium-dependent cell-cell adhesion molecule, in ELCs with a specific neutralizing antibody, SHE 78-7 (5μg/ml), and comparing the invasion of non-treated (NT) and SHE 78-7-treated ELCs into preformed microtracks. Quantification data showed significantly increased invasion of SHE 78-7-treated ELCs (**Figure 4a & 4c**) further along the microtracks (**Figure 4b& 4c**), compared with non-treated ELCs. Without microtracks or HICs, SHE 78-7-treated ELCs remained non-invasive on the side of MAT. However, upon co-culture of SHE 78-7-treated ELCs with HICs, invasion was markedly increased relative to NT ELCs co-cultured with HICs (**Figure 4d**), along with the number of invading ELCs per single HIC (**Figure 4e & 4f**). These data clearly suggest that HICs promote ELC invasion, when cell-cell adhesion in ELCs is suppressed. Moreover, cell-cell adhesion in ELCs is so strong that the cells tend not to migrate along the preformed microtracks, suggesting that other factors influence ELC invasion.

Cell-cell interactions via junction proteins between HIC and ELC are required for ELC invasion

HIC appears to lead the ELC invasion via two main mechanisms: (1) generating microtracks within the matrix that enable ELCs to follow and (2) maintaining cell-cell interactions via junction proteins between the two cell types. Fluorescence-stained cell images disclosed that contact of HICs with ELCs affects induction of ELC invasion alongside microtrack generation (**Figure 5a**). This finding was confirmed by staining with antibodies against tight junction markers, including claudin-5, claudin-1, occludin and E-cadherin. Interestingly, claudin-5, claudin-1 and occludin were expressed in some HICs in close contact with ELCs (as indicated with white arrows), but not in HICs that did not in contact ELCs (indicated with black arrows). Additionally, E-cadherin was weakly expressed in some HICs (indicated with black arrows) (**Figure 5b**). The contact between HIC and ELC influenced on the invasion speed of HICs that directly contacted with ELCs, but it didn't influence on the entire invasion speed of HICs (**Supplementary Figure 3).** This results might carefully suggest that HICs would increase the cell-cell contact between ELCs and vice versa, and enhance their invasion potential by leading collective invasion, resulting in promotion of metastatic potential (**Supplementary Figure 4**).

To confirm whether soluble factors secreted by HICs influence ELC invasion in addition to physical contact, ELCs were cultured on naïve or microtrack- containing MAT in fresh medium or under a gradient of HIC-conditioned medium (**Figure 5c**). Quantification data (**Figure 5c**) showed that soluble factors secreted by HICs do not promote ELC invasion, further verifying that physical contact between the two cell types is essential to stimulate ELC invasion.

Conclusion

Intratumor heterogeneity, where a single tumor colony is composed of multiple subpopulations of cancer cells with distinct molecular and gene expression patterns as well as different phenotypic traits,(7) is one of the leading causes of unpredictable drug efficacy and drug resistance(2). While several studies have been performed to characterize intratumor heterogeneity, the majority are limited to the mechanisms at the molecular and genetic levels, presumably due to the lack of controllable experimental systems that enable precise regulation of cell-cell and cell-ECM interactions in 3D tumor invasion. To our knowledge, the phenotypic characteristics of heterogeneous tumor cell invasion have not been described to date.

In the current study, we established a microfluidic-based tumor heterogeneity *in vitro* model to determine the phenotypic characteristics, including morphology, and proliferative, invasive, and metastatic potentials, of heterogeneous cell subpopulations in a single tumor colony during tumor progression. Since the ECM within tumors is also heterogeneous, cancer cells need to overcome ECM barriers for successful metastasis(18, 19). To escape the original tumor mass and invade surrounding tissue, cancer cells display plasticity by employing various strategies, including changes in migration patterns (from collective to single motility)(18, 20) and proteolytic ECM remodeling(21, 22). In contrast, cancer cells that retain epithelial characteristics mostly grow in place, but to escape from the original tumor colony and metastasize, they need to recruit and allow stromal cells to deposit and remodel ECM(23) or undergo epithelial-mesenchymal transition (EMT)(24, 25). Since many tumors frequently display intratumor heterogeneity, invasive and epithelial-like cancer cells co-exist within a single tumor colony, implying reciprocal effects of these cells to stimulate tumor progression. In our tumor heterogeneity model, HICs stimulated the invasive potential of ELCs with proteolytic ECM remodeling and maintenance of cell-cell physical contact. Microtracks within the matrix generated by ECM proteolytic activity of HICs were required to promote the collective invasion of ELCs. Additionally, physical contact of HICs with ELCs, in conjunction with microtrack generation, promoted ELC invasion via expression of junction markers, such as claudin 1&5, occludin, and E-cadherin.

Stromal cells, such as tumor-associated fibroblasts, promote carcinoma growth and invasion by depositing and remodeling ECM around tumor and secreting growth factors(23, 26). Moreover, fibroblasts have been shown to lead collective carcinoma cell invasion(17). Here, we have shown for the first time that mutual cooperation of subpopulations in heterogeneous tumors stimulates metastatic potential, with HICs acting as leaders and ELCs as followers. ELC invasion activity was sufficiently induced by the combination of microtrack generation and maintenance of physical contact with HICs with no stromal cells or genetic alterations.

Acknowledgments

S.Chung was supported by the NRF (NRF) grant funded by MEST (No. 2013R1A2A2A03016122), by the Human Resources Program in Energy Technology of the KETEP grant financial resource from the Ministry of Trade, Industry & Energy, Republic of Korea (No. 20124010203250), and by Basic Science Research Program through the NRF of Korea funded by the Ministry of Education, Science and Technology (grant number: 2012-022481). E. Chung was supported by the Bio & Medical Technology Development Program (No. 2011-0019633) and by the Basic Science Research Program (No. 2012R1A1A1012853) of the NRF funded by MEST. The authors thanks Ms. Deokyeon Jo for help with experiments.

1. A. Marusyk, V. Almendro and K. Polyak, Nature Reviews Cancer, 2012.
2. S. J. Diaz-Cano, International journal of molecular sciences, 2012, 13, 1951-2011.
3. W. G. Stetler-Stevenson, Cancer and Metastasis Reviews, 2008, 27, 57-66.
4. H. F. Dvorak, V. M. Weaver, T. D. Tlsty and G. Bergers, Journal of surgical oncology, 2011, 103, 468-474.
5. T. A. Yap, M. Gerlinger, P. A. Futreal, L. Pusztai and C. Swanton, Sci Transl Med, 2012, 4, 127ps110.
6. L. L. Campbell and K. Polyak, Cell Cycle, 2007, 6, 2332-2338.
7. S. Bhatia, J. V. Frangioni, R. M. Hoffman, A. J. Iafrate and K. Polyak, Nature biotechnology, 2012, 30, 604.
8. A. Marusyk and K. Polyak, Biochimica et Biophysica Acta (BBA)-Reviews on Cancer, 2010, 1805, 105-117.
9. B. Weigelt, J. L. Peterse and L. J. van't Veer, Nature reviews cancer, 2005, 5, 591-602.
10. I. J. Fidler, Cancer Research, 1978, 38, 2651-2660.
11. T. D. Tlsty and L. M. Coussens, Annu. Rev. Pathol. Mech. Dis., 2006, 1, 119-150.
12. H. J. Knowles and A. L. Harris, Breast Cancer Res, 2001, 3, 318-322.
13. M. Egeblad, E. S. Nakasone and Z. Werb, Developmental cell, 2010, 18, 884-901.
14. M. Snuderl, L. Fazlollahi, L. P. Le, M. Nitta, B. H. Zhelyazkova, C. J. Davidson, S. Akhavanfard, D. P. Cahill, K. D. Aldape and R. A. Betensky, Cancer cell, 2011, 20, 810-817.
15. M. Shipitsin, L. L. Campbell, P. Argani, S. Weremowicz, N. Bloushtain-Qimron, J. Yao, T. Nikolskaya, T. Serebryiskaya, R. Beroukhim and M. Hu, Cancer cell, 2007, 11, 259-273.
16. M. Shackleton, E. Quintana, E. R. Fearon and S. J. Morrison, Cell, 2009, 138, 822-829.
17. C. Gaggioli, S. Hooper, C. Hidalgo-Carcedo, R. Grosse, J. F. Marshall, K. Harrington and E. Sahai, Nature cell biology, 2007, 9, 1392-1400.
18. Y. Shin, H. Kim, S. Han, J. Won, H. E. Jeong, E. S. Lee, R. D. Kamm, J. H. Kim and S. Chung, Advanced healthcare materials, 2012.
19. A. R. Anderson, A. M. Weaver, P. T. Cummings and V. Quaranta, Cell, 2006, 127, 905-915.

20. S. Giampieri, C. Manning, S. Hooper, L. Jones, C. S. Hill and E. Sahai, Nature cell biology, 2009, 11, 1287-1296.

21. P. Friedl and S. Alexander, Cell, 2011, 147, 992-1009.

22. P. Friedl and K. Wolf, Nature Reviews Cancer, 2003, 3, 362-374.

23. R. Kalluri and M. Zeisberg, Nature Reviews Cancer, 2006, 6, 392-401.

24. H. Hugo, M. L. Ackland, T. Blick, M. G. Lawrence, J. A. Clements, E. D. Williams and E. W. Thompson, Journal of cellular physiology, 2007, 213, 374-383.

25. J. P. Thiery, H. Acloque, R. Y. Huang and M. A. Nieto, Cell, 2009, 139, 871-890.

26. N. A. Bhowmick, E. G. Neilson and H. L. Moses, Nature, 2004, 432, 332-337.

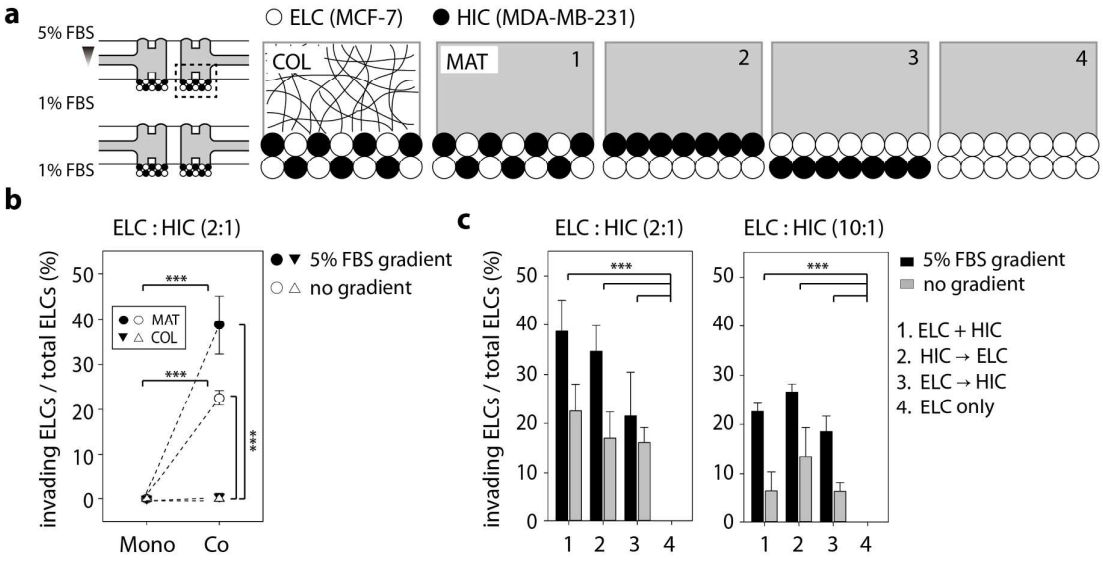

Figure 1. **A tumor heterogeneity *in vitro* model.** (a) Schematic representation of the heterotypic co-culture system for studying cancer invasion in intratumor heterogeneity. ELCs/HICs were co-cultured on COL and MAT under a FBS gradient or no gradient. Moreover, ELC/HICs were cultured on MAT via a different seeding technique (#1~#4). (b) Quantification of ELC invasion into COL and MAT in the presence or absence of HICs under a 5% FBS gradient or no gradient in the tumor heterogeneity model. Mono and Co represent mono-culture and co-culture, respectively. (c) Quantification of ELC invasion into MAT with a different seeding order (#1~#4) at seeding ratios of 2:1 and 10:1 (ELC:HIC) in the absence or presence of FBS gradient. All data are expressed as mean ± SD. ($n > 4$, ***$p < 0.001$)

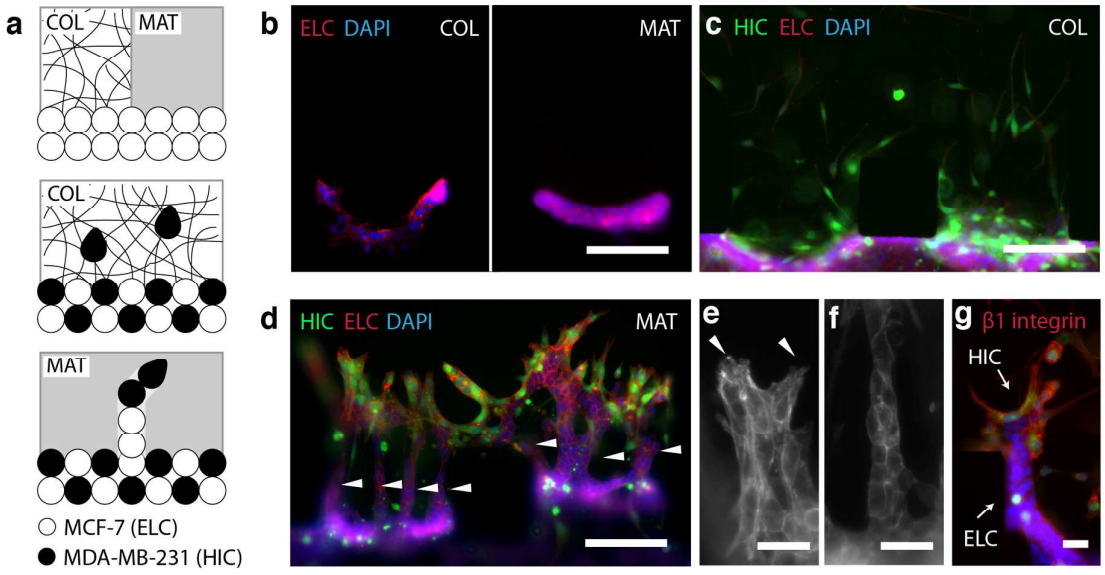

Figure 2. **HIC promotes ELC invasion into MAT, but not COL.** (a) Simple depiction of ELC invasion into COL and MAT in the absence and presence of HIC. Representative images of (b) ELC (red) invasion into COL and MAT in the absence of HIC (green) and ELC (red) invasion into (c) COL and (d) MAT in the presence of HIC (green). (e) Representative images of invading morphologies of HIC and (f) ELC into MAT (F-actin staining). (g) β1 integrin (red) antibody staining of invading HICs (green) and ELCs and white arrows indicate HICs and ELCs. Scale bar: (b)(c)(d) 150 μm, (e)(f)(g) 35 μm

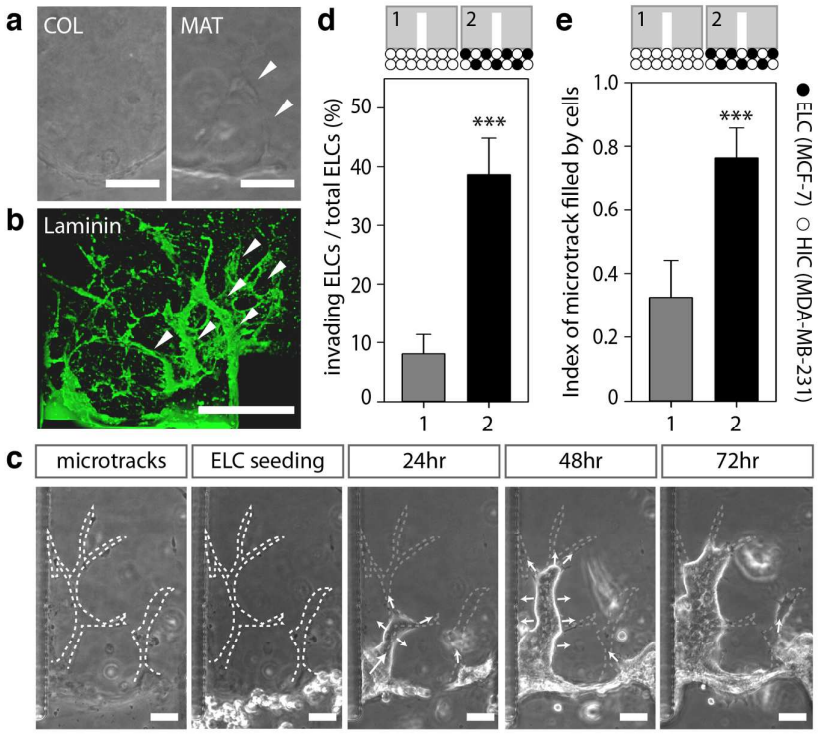

Figure 3. **HIC remodels ECM and generates microtracks within the matrix (MAT but not COL).** (a) COL and MAT matrices after extraction of invading HICs. White arrows indicate microtracks within MAT. (b) Remodeled ECM stained by anti-laminin antibody (green). The inner surfaces of microtracks are more richly stained (indicated by white arrows). (c) Phase-contrast image of remodeled MAT containing microtracks generated by HICs and time-lapse images of ELC invasion into microtracks under 5% FBS gradient. (d) ELCs were cultured in remodeled MAT in the absence and presence of HIC. Quantification of ELC invasion along microtracks in the absence and presence of HIC and (e) quantified index of microtracks filled with ELCs after three days of culture. All data are expressed as mean ± SD. ($n > 8$, ***$p < 0.001$)

Scale bar: (a) 75 μm, (b) 150 μm, (c) 50 μm

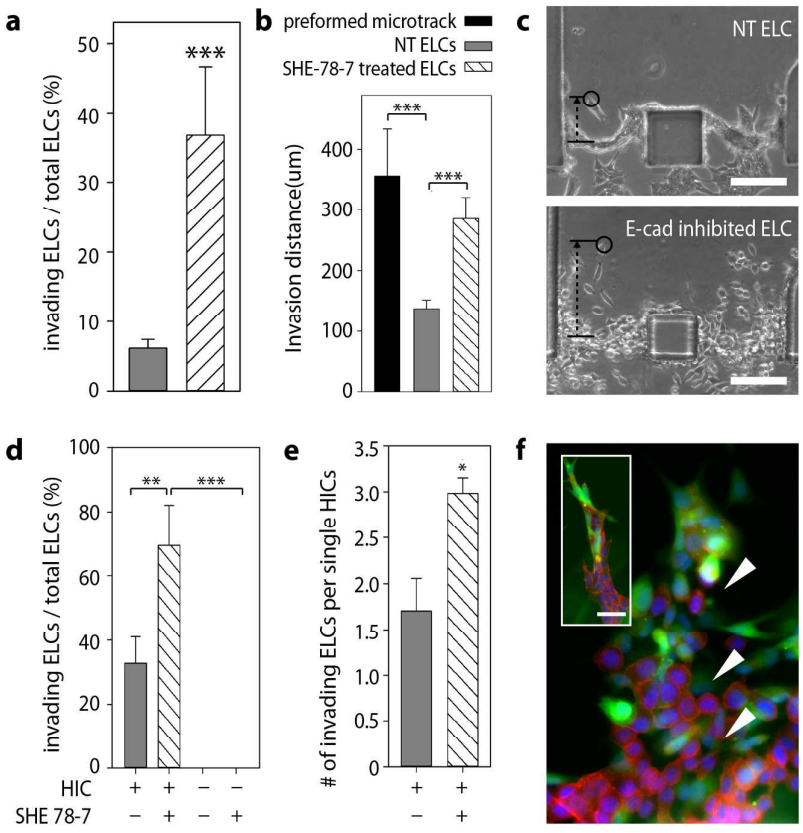

Figure 4. **Microtracks in ECM are insufficient for promoting considerable amount of ELC invasion.** (a) Percentage invasion of non-treated and SHE 78-7-treated ELCs into preformed microtracks. (b) Comparison of the length of microtracks within MAT with the invading distance of non-treated and SHE 78-7-treated ELCs. Black bar represents the length of preformed microtracks. (c) Representative images show that ELCs treated with SHE78-7 invaded further along microtracks into MAT than non-treated ELCs. (d) Quantification of ELC invasion in the absence and presence of HIC or following treatment with SHE 78-7. (e) Quantification of invading ELCs per single HIC. (d) Invasion of ELCs treated with SHE78-7 into MAT in the presence of HICs. The small image shows non-treated normal ELC invasion into MAT in the presence of HIC. Green indicates HIC, red signifies ELC and white arrows show ELC invasion led by HIC. All data are expressed as mean ± SD. ($n > 4$, $*p < 0.05$, $**p < 0.01$, and $***p < 0.001$)

Scale bar: (c) 150 μm and (f) 50 μm (small image), 150 μm (big image)

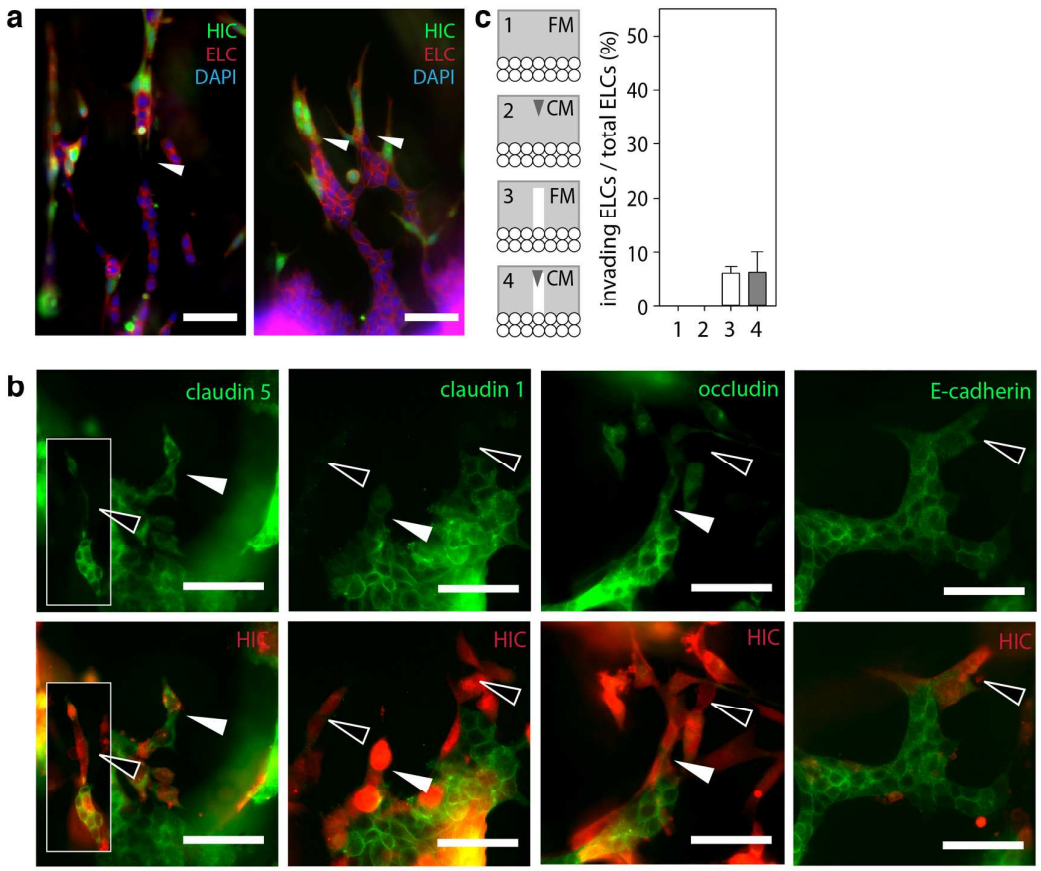

Figure 5. **Physical contact between HICs and ELCs facilitates ELC invasion into ECM** (a) Two mechanisms underlying HIC activity as leaders for ELC invasion. HIC (green) promoted ELC (red) invasion by generating microtracks (white arrows in the left image) and maintaining cell-cell contact with ELC (white arrows in the right image). (b) Representative image of the junction marker expressed in HICs. White arrows indicate the expressed junction markers in HICs and black arrows indicate non-expressed junction markers in HICs. (c) Quantification of ELC invasion into non-remodeled and remodeled MAT in fresh medium (FM) or under a gradient of HIC-conditioned medium (CM) (#1~#4). (n =6) All data are expressed as mean ± SD. Scale bar: (a) 30 μm, (b) 75 μm